

<Review>

Anodic Film Formation on Aluminum (I) - Anodic Film Morphology -

Seong-Ho HAN

Surface Engineering Laboratory Korea Institute of Machinery and Metals,
Changwon, Kyungnam, Korea

양극산화 피막형성에 관한 연구 (I) - 양극 산화 피막 구조 -

한 성 호

한국 기계 연구소
포면 공학 연구실

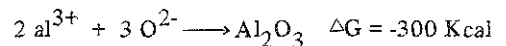
초 록

최근에 와서 알루미늄 소재의 양극산화피막 형성 Mechanism에 관한 연구는 응용분야의 폭이 넓어지면서 많은 연구가 진행되고 있다. 최신 분석 장비의 응용의 폭이 넓어짐으로 해서 연구의 깊이도 점차 증가되고 있는 실정이다. 따라서, 선진국의 양극산화피막에 관한 연구는 어디까지 왔는가를 조망하므로 해서 그 응용의 기반을 확고히 하기 위해 본 Review를 연재하고자 한다. 본고에서는 가장 기본적인 연구과제인 양극산화피막의 Morphology에 관한 내용이다.

1. Introduction

Any literature review concerning anodizing in aqueous solution must first start with an up to date appraisal of the anodic films themselves, including their morphology, structure, composition and growth mechanisms. When aluminium is anodically polarized in a certain electrolytes, with a suitable metal or carbon counter electrode completing the cell, the thin surface air formed oxide film can be thickened greatly to form the resultant anodic film. Here, the term anodic oxide film is not used to describe the product of anodizing since, even though the film comprises essentially Al_2O_3 , there is also incorporation of varying amounts of the electrolyte anion from the anodizing electrolyte, the extent

depending on the anion-type and anodizing conditions, and water, which may be free and bound. The oxidation process can be represented classically as shown below³;



The type of anodic film produced is dependent on several factors^{1,6} including electrolyte type, anodizing current density, pH and temperature^{2,4}. The films are usually classified as barrier and porous anodic films. More generally, Tajima³ has identified at least five types of voltage time behaviour apparent during anodic polarization of aluminium in various aqueous electrolytes at constant current density, as shown in Figure 1.1:

1. Barrier-type anodic film formation in electrolytes in which the film is only barely soluble, for instance, neutral borate, or tartrate electrolytes in the pH range 5-7, phosphate, and citrates. Generally, the cell voltage rises approximately linearly with time from the commencement of anodizing until dielectric breakdown occurs at a relatively high voltage value. Apart from the temperature of the electrolyte, the barrier-type film thickness is controlled solely by the voltage applied, and the maximum film thickness is restricted to a voltage below the dielectric breakdown voltage value, i.e., 500-700V, which corresponds to a film thickness in the region 700-1000nm.
2. Porous anodic film formation is apparent in certain acid and alkali electrolytes in which the resultant film is termed "sparingly

soluble", e.g. sulphuric acid, phosphoric acid, chromic acid, and oxalic acid. Generally the cell voltage rises with time from the commencement of anodizing to a maximum voltage, and subsequently declines to a relatively constant, steady-state voltage for the duration of the run.

3. Pitting by metal dissolution can compete with anodic film formation in certain organic acid electrolytes, in neutral sulphate electrolytes, and in electrolytes containing chloride ions. Generally the cell voltage is seen to rise to a maximum value before declining gradually.
4. A situation employed in electropolishing in appropriate strong acids where the film dissolves almost as soon as it forms. The cell voltage may fluctuate periodically or remain steady at a relatively low level during electropolishing.
5. When much of the surface oxide film is removed by crystallographic etching in certain strong acids, halides and alkaline electrolytes, the identical cell voltage established is very low and it remains at a constant level.

The monitored voltage-time transients, and current-time transients for anodic polarization at constant voltage, represent the summation of the behaviour generally over the surface and of processes occurring at flaws, and there is some overlap in the classification listed above. Borderline behaviour may occur over an entire specimen surface or two or more processes may occur on a single surface. The following sections are concerned with morphology, composition and structure of barrier-type and porous-type anodic films.

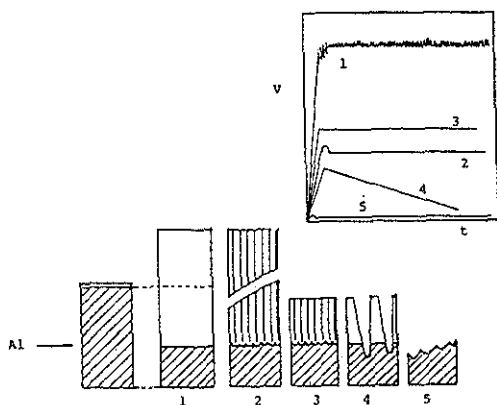


Fig. 1 Voltage-time characteristics for anodizing at constant current density and the corresponding surface structure; from Taiima (3); (1) barrier-film formation type, indicates scintillation by electrical breakdown of the anodic film (2) porous film formation type; (3) electropolishing type; (4) anodic pitting type; (5) anodic etching type.

2. Barrier-type Anodic Films

During anodizing of aluminium under conditions which favour barrier film formation, and at a constant current density, the voltage across the cell rises approximately linearly with time. The limiting voltage attained while anodizing at constant current density is determined by the electrical breakdown voltage, which can vary from 40V to approximately 700V, depending primarily on the electrolyte type and concentration⁸. The linear voltage rise prior to breakdown stems from the field strength i.e. the ratio of applied voltage to film thickness, necessary to allow ionic migration and hence film growth, which is found to be between 10^6 – 10^7 V cm⁻¹. Therefore, under constant voltage anodizing, the current density remains at a relatively high level until the film thickness is attained, thereafter, when the field strength falls to approximately 10^6 V cm⁻¹, ionic movement is limited and further film growth ceases. At this stage, the current density reduces to a very low value, termed the 'leakage' current, which is normally attributed to electronic conduction, probably at flaws in the film⁹ or, arguably, controlled within the bulk of the film¹⁰. Flaws or weak spots always exist in barrier film, of population densities between 10^8 – 10^{14} m⁻² and are associated with the substrate topography^{11,12}, the presence of impurities on the substrate surface¹³ and the anodizing conditions¹⁴. The film thicknesses can be quoted in terms of its unit thickness and applied voltage, which is expressed generally in nmV⁻¹; such values can range between about 1.2–1.4 nm V⁻¹⁵ and depend mainly on the

electrolytes used and also, to a limited extent, on the anodizing temperature, electrolyte concentration and current density^{15,16}.

Transmission electron microscopy (TEM) of ultramicrotomed sections of the film material attached to the substrate has shown that the films are relatively uniform in thickness, relatively compact, and apparently featureless within the resolution of the microscope. Stripped films when viewed in plan in the TEM, are also featureless, indicating no surface roughness per se, although they do reproduce the original substrate topography¹⁷. However Franklin¹⁴ observed evidence, under certain conditions, of a cellular structure existing in the barrier film formed to high voltages at 293 K in a boric acid-borate electrolyte. He considered that the film contained three types of material, mostly amorphous alumina, with different extents of crystallinity and a hydrated alumina outer layer, which showed a different dissolving power in the film stripping solution employed. The proportions of the three types of material varied as the formation temperature of the anodizing electrolyte changed. Recently, Thompson et al¹³ employed direct observation techniques to determine the location, and the precise morphology of the crystalline material enabling its mechanisms of formation to be elucidated. Recent work by Shimizu, Tajima, Thompson and Wood¹⁸ showed the formation and development of local regions containing γ' - crystalline alumina surrounding flaws in anodic barrier films formed on aluminium in aqueous ammonium borate electrolytes at room temperature. The formation of crystalline alumina islands at these localized sites become more

readily evident when the forming voltage approached about 100V and they grew radially with further increase in the forming voltage. The islands of crystalline alumina were thought to form by a thermal conversion of the original barrier film formed by the usual ionic processes, due to local Joule heating effects. The radial growth of the islands and their population density were influenced by increase of bulk temperature of the electrolyte, but was almost unaffected by the concentration of the electrolyte and applied anodizing current density. Typical flaw, and resultant enveloping crystalline island population densities are about $2.4 \times 10^{12} \text{ m}^{-2}$, which decrease with chemical cleaning and electropolishing pretreatments of the aluminium substrate to about 3.7×10^{11} and 10^9 m^{-2} respectively. Such data indicate the role of impurities, and associated flaws rather than substrate topography per se, on the development process, although the initial role of impurities is likely to be intimately bound up with topographical features. The estimated values of the population density of flaws agreed with work by Shimizu and Tajima¹⁹ and Thompson, Shimizu and Wood¹³.

Richardson, Wood and Sutton²⁰ classified flaws into two types, termed residual and mechanical flaws. Residual flaws were thought to arise from regions of impurity segregation on the original substrate surface, while mechanical flaws originated from gross structural defects such as scratches or relatively rough regions of the surface. They quoted flaws as having diameters between 1 and 400nm and population densities in the range 10^8 to 10^{14} m^{-2} . More recently flaws have been considered as having

a wide variety of sizes, shapes, numbers and states of activity²¹, with little real distinction between mechanical and residual flaws. Vermilyea^{22,23} studied barrier films formed on several valve metals including aluminium, but mainly on tantalum. Estimated flaw population densities were in the range 10^8 – 10^{12} m^{-2} , the lowest population density of flaws being associated with a chemically polished surface and the largest density with an abraded surface; interestingly not all such flaws were thought to be in intimate contact with the substrate, i.e. they did not all open to physical holes upon polarization in various environments. The dimensions quoted were relatively large, and for a film of thickness 240nm the effective diameter of the flaw was 300nm.

Doherty et al⁹, in a study of pit initiation on aluminium substrates of controlled cellular texture, supporting an air-formed film, produced evidence to suggest that persistent, active flaws in the film exist above the triple point in the underlying substrate, present where three cells meet. For the pre-conditioned substrate employed this indicated 10^{13} m^{-2} flaws, although re-passivation of the less active flaws under the conditions used reduced the number of flaws which developed into pits to about 10^{10} m^{-2} . In relation to previously quoted flaws population densities, this also implies that the thinner the film the greater the apparent flaws population density.

Dorsey^{24,25,26} has employed infra-red, impedance and later transmission electron microscopy techniques in order to gain further insight into the structure and composition of films formed in 2M boric acid (pH 4.5) at 333K,

and to provide evidence of the duplex film structure suggested previously. The inner layer was a supposedly primary phase barrier layer, about 20nm thick and independent of the formation voltage. However, a pronounced increase in thickness of the outer layer was found, while the layer adjacent to the metal surface remained consistent with the 1.4nm V^{-1} relationship, when the anodizing temperature was increased to 363K. The reliability and resolution given by infra-red data have been questioned by other workers^{2,12,13}. Leach and Neufeld²⁷ observed that the barrier film, formed in borate electrolyte (pH 9.7), showed typical barrier morphology at ambient temperature and a definite porous morphology at higher temperatures. Randall and Bernard²⁸ reported that the current efficiency of anodic film formation in aqueous phosphate electrolyte decreased with increasing current density, decrease of stirring rate and of electrolyte pH, when the current efficiency was below about 85%, transmission electron micrographs showed development of typical porous film networks, but no clear line of demarcation was established between porous and barrier-type films. Takahashi and Nagayama²⁹, Choo and Devereux³⁰, and Hoar and Yahalom³¹ also observed similar porous morphologies in films formed in borate and tartrate electrolytes after prolonged anodizing at constant potential. The rate of growth of the outer porous film increased as the anodizing temperature increased.

3. Porous-type Anodic Films

The morphology of porous anodic films,

formed on aluminium in aqueous electrolytes, has been extensively documented^{2,4}; some important aspects are considered below, with particular reference to recent advances in the methods of investigating surface films.

In certain electrolytes, in which the resultant anodic film is sparingly soluble, porous film growth takes place. Porous anodic films have duplex morphologies, i.e. an outer region of relatively thick and regular porous film material, which lies above the thin, more compact barrier layer region adjacent to the metal/film interface. The thickness of the inner barrier layer region is directly dependent on the voltage, similar to the barrier-type anodic film, whereas the outer porous layer thickens coulombically. Although there are differences between barrier-type and porous-type anodic films, the border line in the forming conditions is not quite distinct. Much of the previous section concerning barrier-type films is relevant to the following review of porous-type films, the fact that both porous and barrier-type films can generally be formed in the same electrolyte having already been stated.

Regular porous anodic films can be formed in acid^{32,38}, neutral^{29,31} and alkaline electrolytes^{39,41}; acid electrolytes are most commonly employed and this survey refers to such cases, typically in sulphuric acid^{33,38}, oxalic acid^{36,42}, chromic acid^{33,37} or phosphoric acid^{32,34,35}. The acid electrolytes generally give relatively uniform porous film growth over the macroscopic metal surface, for a wide range of anodizing conditions.

Since the first observation of the porous film by Setoh and Miyata⁴³, in 1932, many workers have proposed different models relating

to the morphology of porous film.

An early model of the porous film, which gained popular support, was presented by Keller, Hunter and Robinson⁴⁴; this is shown schematically in figure 1.2. The essential points of this model are that the porous film consists of numerous identical units, predominantly hexagonal in shape, termed 'cells', each containing a single pore which passes approximately perpendicular to the metal substrate. Each cell contains one star shaped pore at its centre which was separated from the aluminium substrate by a scalloped barrier layer. The proposed pore shape is that of a six-pointed star due to a differential dissolution effect caused by the geometry of the enveloping hexagonal cell. Measurements from films formed under various conditions gave a cell size proportional to the forming voltage with typical measured values in the range of 40-280 nm. Barrier layer thickness to voltage ratios of 1.10, 1.09, 0.97 and 0.80 nm V⁻¹ were determined from the cell diameter and pore diameter in 4% phosphoric, 3% chromic, 2% oxalic and 15% sulphuric acids respectively; the corresponding pore diameters were 33, 24, 17 and 12 nm. They concluded that the cell wall thickness and barrier layer thickness were primarily a function of the cell voltage, while the pore diameter was dependent on the electrolyte concentration and temperature. This last point has since been shown to be an erroneous conclusion⁴⁵. Furthermore, star-shaped pores have not been observed in the section of the films examined directly.

Hunter and Fowle^{46,47} showed that the barrier layer thickness was time independent

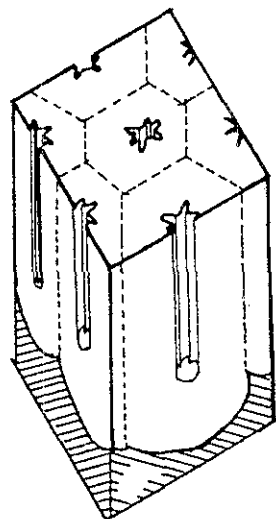


Fig. 2 Schematic illustration of the porous anodic film proposed by Keller and Robinson (44)

and was proportional to the applied voltage for the porous films formed. They used an electrical method, involving reanodizing of the substrate and its film in the major anodizing acids, i.e. sulphuric, oxalic, chromic and phosphoric acids. The unit barrier layer thickness usually expressed in nm V⁻¹) was dependent on electrolyte type, concentration and electrolyte temperature. For non-aggressive electrolytes, the unit barrier thickness was quoted as 1.4 nm V⁻¹, while the solvent action of aggressive electrolytes appreciably reduced this value. They reported values of 1.00, 1.18, 1.19 and 1.25 nm V⁻¹ for films formed in 15% sulphuric acid at 283K, 2% oxalic acid at 300K, 4% phosphoric acid at 300K and 3% chromic acid at 315K. The unit barrier layer thickness decreased with increase of temperature and at a greater rate with decrease of acid concentration.

Adsorption techniques for measurement of pore volume, which is defined as the percentage of fractional volume of the film occupied by pores, were used by Paolini and his co-workers⁴⁸ and Mason⁴⁹. When the pores were assumed as perfect smooth cylinders, calculation of pore diameters gave values which were in conflict with previous estimates⁴⁴; thus, a pore wall roughness factor was introduced. They suggested that the pore volume was a function of the porous film thickness, current density, electrolyte concentration, and anodizing temperature. The pore shape was thought to be a truncated cone due to chemical dissolution of the cell material in the electrolyte.

The above studies were based on surface topography of anodic films, involving replication and direct transmission electron microscopy of stripped films and some chemical adsorption techniques. The first direct electronmicroscopy observation from the polished section of a porous anodic film was reported by Booker, Wood and Walsh^{50,51}. A polished section of film, formed in 17.5% sulphuric acid, was observed, which showed the pores present in small craters, usually close to the edges of the film, where pieces of film had been disrupted. The bulk of the film sections, after polishing, showed a 'rain drop' pattern where pores, not quite parallel to the polishing direction, were revealed. From these observations more accurate values of the pore diameters were obtained. Pore diameters were in the range 15-20 nm for films formed at 100 Am^{-2} , with pore centres 59-60 nm apart. The pore diameters showed little variation throughout the film thickness and any variation in the current density was

shown to change the cell base pattern, suggesting a similar change in the porous morphology.

Later, Murphy and Michelson⁵², after examining critically previous models, suggested a different model of the porous anodic film based on a colloidal chemistry point view. They claimed that the pores, seen in the electron microscope or deduced from gas adsorption experiments, could be due, at least partly, to the drying out process of the film involved necessarily during specimen preparation or examination under low pressure conditions. Their model was more related to the film microstructure rather than the film morphology for which they did not raise any objection to Keller, Hunter and Robinson's model. The model is reviewed in part (II) of this series.

Apart from the morphology proposed by Keller, Hunter, and Robinson⁴⁴, several other studies have been reported, the results of which have been suggested to reveal a basic inconsistency in the cylindrical pore model. Czokan^{53,54} in an investigation of hard anodic oxide films on aluminium, i.e., those films formed at low temperature and usually in dilute sulphuric acid, has reported that the pore morphology is not as regular as was previously believed. The morphology observed was one in which the pore distribution was irregular and where the pores themselves were twisted and bent or otherwise distorted. The occurrence of a high density of pore openings at the surface appeared to produce a fibrous structure, whose size, shape, and orientation varied considerably. Under polarized light, a laminar structure was observed parallel to the metal surface, which tended to agree with the earlier model of Murphy

and Michelson⁵². Aluminium subgrain structure was suggested to influence, at least partially, the orientation of the groups of pore channels. That pore colonies can occur at some preferred sites has already been suggested by Renshaw⁵⁵. Ginsberg and Wefers^{56,57} suggested that the films had a regular fibrous structure, which is different from the irregular fibrous structure model of Csokan⁵³, with individual fibres being 20-50nm in diameter and having approximately similar radii to the cell and pore of earlier models. Groups of fibres, about 1µm in diameter and usually conical in appearance, were observed in the optical microscope. Film porosity was due to the partially hollow fibres and inter-fibre space, while the barrier layer existed where the fibres grew together from the metal.

Several studies have been made to determine the variation of film parameters with anodizing conditions in a quantitative way. The dependence upon cell voltage and current density was established for normal anodic films^{45,58}, while further work has been performed on hard anodic films^{54,59}. Tomashov and Zalivalov⁵⁹ reported that both hardness and wear resistance were dependent upon the porosity of the porous film. Hard anodic films formed at 22-27 V in 14 N H₂SO₄ at 273.5K showed no detectable pore widening with thickness of the film, and porosity was about 4% compared with 16% for normal films^{44,60,61}. Corresponding cell population densities were 435 and 295×10¹² cells m⁻² for 'normal' and 'hard' films respectively.

O'Sullivan and Wood⁴⁵ reached certain conclusions about the film morphology from the direct observation of carbon replicas of

fracture sections and stripped films, formed at constant voltage in phosphoric acid under specific anodizing conditions. From a large number of measurements of the major film parameters, such as the thickness of the barrier layer, the pore diameter, the cell size and the curvature of pore and cell bases, they concluded that the cell diameter, barrier layer thickness and, contrary to Keller et al⁴⁴, pore diameter, were all directly dependent on the anodizing voltage. A schematic representation of their model, showing the parallel-sided cylindrical pores, instead of star-shaped sections, passing perpendicular to the aluminium substrate, but separated from it by a barrier layer with its scalloped appearance, is shown in Figure 1.3. One of their major findings was that a relationship exists between the curvature of the cell and pore base and the current distribution across the barrier layer. Using this model, the mechanism proposed for controlling film growth in the steady-state region was the dynamic balance between film growth at the barrier layer and field assisted dissolution, suggested by Hoar and Mott⁶², aided by local temperature rises at the pore base. Field assisted dissolution is reconsidered further in part (III) of this series.

The current 'recovery effect' has been studied by many workers^{45,52,63}. The recovery effect is produced when the formation voltage is changed suddenly. After a sudden reduction in cell voltage, the current decreased initially, followed by a relatively long time duration of current recovery to proceed to the new equilibrium current corresponding to the new lower voltage. Murphy and Michelson⁵² re-

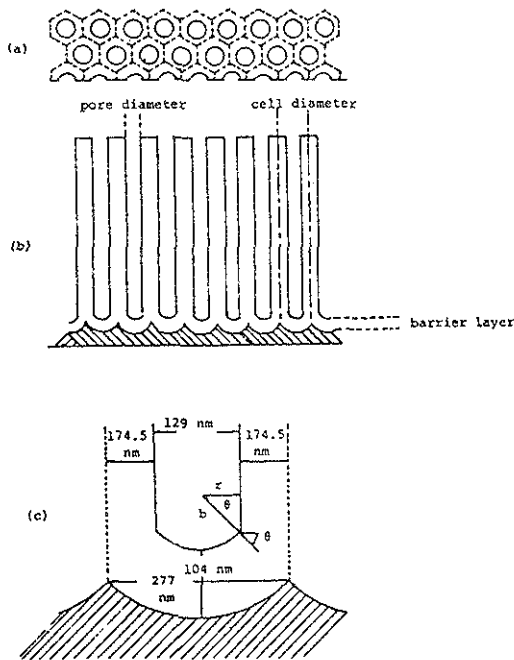


Fig. 3 Schematic illustrations of the porous anodic film, reported by O'Sullivan Wood⁽⁴⁵⁾; (a) plan view (b) sectional; (c) detailed representation of the barrier layer, cell material and the pore of a steady-state porous anodic film, developed on aluminium at 100V in phosphoric acid.
 r = pore diameter; b = pore base radius curvature. $\cos^{-1} \theta = r/b$ = cell thickness/barrier thickness

ported that no change of the geometrical structure of the film would occur during the low current stage until the current started increasing, when physical thinning of the barrier layer occurred. They indicated that this was inconsistent with the Keller et al⁴⁴ model. However, O'Sullivan and Wood⁴⁵, Diggle et al⁶⁸, and Takahashi et al⁶³, all concluded that thinning occurred as soon as the voltage dropped. The change in the film morphologies, before and after the current recovery, showed clearly the dependence of the resultant film parameters

on the anodizing voltage. For a sudden decrease in anodizing voltage, a pore branching model was proposed to describe the morphological changes during the current recovery process⁶³. The work by Renshaw⁵⁵, using electron microscopy reveals that the porous film develops from the branching of isolated surface pores with the formation of colonies of pores beneath the preformed barrier-type film. The colonies comprise relatively uniform, hemispherical arrays of pore-containing cells, which at various stages, grow by continual branching of the pore structure and so spread laterally over the specimen surface, as well as into the metal. Thompson and Wood⁶⁴ and Bailey³³ have studied porous films formed in chromic acid. They found that although the general porous film model was valid, several anomalous features were also evidence; the pores were not always normal to the substrate and pore branching often occurred through the film thickness. The cell wall was relatively irregular with many feather-like regions penetrating the cell material from the pore well. After careful scrutiny of pore sections, Bailey³³ suggested that the peculiar morphology apparent to a 'self-sealing' effect usually took place at bulk solution temperature over 363K. Ono, Chiaki and Sato found similar features and suggested a phenomenological model termed the 'branching colonial pore structure'.

Recently Thompson et al^{38,66} examined directly in plan porous anodic films which had been ion beam thinned from both sides. They noted irregular pore section shapes, which were somewhat reminiscent of the starshaped pore model proposed by Keller et al⁴⁴, and a

distorted cellular morphology apparent in the films formed in sulphuric, oxalic, chromic and phosphoric acids. More recently Tan⁶⁷ examined the morphology of the cells, pores and the barrier layers comprising the anodic films formed on aluminium using TEM of ion beam thinned films and carbon replicas of film fracture sections. From this work, the major anodic film parameters were proportional to the anodizing voltage as expected, but the arrangement of the film material into cells with their regions of different texture and composition, was far from regular. Tan also concluded that the cells attempted to develop an hexagonal pattern or arrangement, but this rarely approached true perfection.

REFERENCES

1. S. Wernick, and R. Pinner, "The Surface Treatment of Aluminium and its Alloys", 4th Ed. Robert Draper Ltd., Teddington, (1972).
2. G.E. Thompson, and G.C. Wood, "Corrosion: aqueous processes and passive film". (Treatise on material science and technology; V.23) Ed. J.C. Scully, 205, Academic Press Inc. (London), 1983.
3. S. Tajima, "Advances in Corrosion Science and Technology". Vol. 1. p229, Ed. M.G. Fontana and R.W. Staehle, Plenum Press, New York, (1980).
4. J.W. Diggle, T.C. Downie, and C.W. Goulding, Chem. Rev., 69, (1969) 365.
5. L. Young, "Anodic Oxide Films" Academic Press, London, (1961)
6. G.C. Wood, "Oxide and Oxide Films" Vol.2, p.167, Ed. J.W. Diggle, Marcel Dekker Inc., New York (1973).
7. A.J. Arvia, and N.R. de Tacconi, Thin Solid Films, 43, 173 (1977).
8. S. Ikonipisov, Electrochem. Acta, 22, (1977) 107.
9. P. Doherty, G.E. Thompson and G.C. Wood, J. Electrochem. Soc., 129, (1982) 1515.
10. I. Mizuki, N. Baba and S.J. Tajima, Metal Finish. Soc. Japan, 28, (1977) 30.
11. G.C. Wood, W.H. Sutton, J.A. Richardson, T.N.K. Riley and A.G. Matherbe, In "Localized Corrosion", pp.526-546. NACE-3, Houston (1974).
12. J.A. Richardson and G.C. Wood, J. Electrochem. Soc. 120, (1973) 193.
13. G.E. Thompson, K. Shimizu and G.C. Wood, Nature, London, 286, (1980) 471.
14. R.W. Franklin, In "Proceedings of a Conference on Anodizing", Nottingham, pp.96-100, Aluminium Development Association, London (1962).
15. G. Hass, J. Opt. Soc. Amer., 39, (1949) 532.
16. M.A. Barrett and A.B. Winterbottom, 1st Inst. Cong. on Met. Corrosion, 1961, A.D.A. London (1962), p.96.
17. R.C. Furneaux, G.E. Thompson and G.C. Wood, Corrosion Sci., 18, (1978) 853.
18. K. Shimizu, S. Tajima, G.E. Thompson and G.C. Wood, Electrochim. Acta, 25, (1980) 1481.
19. K. Smizu and S. Tajima, Electrochim. Acta, 25, (1980) 259.
20. J.A. Richardson, G.C. Wood and W.H. Sutton, Thin Solid Films, 16, (1973) 199.
21. M. Janik-Czachor, G.C. Wood and G.E.

- Thompson, Br. Corrosion J., 15, (1980) 154.
22. D.A. Vermilyea, J. Electrochem. Soc., 110, (1963) 250.
23. D.A. Vermilyen, J. Appl. Phys. 36, (1965) 3663.
24. G.A. Dorsey, J. Electrochem. Soc., 113, (1966) 169.
25. G.A. Dorsey, J. Electrochem. Soc., 113, (1966) 172.
26. G.A. Dorsey, J. Electrochem. Soc., 116, (1969) 466.
27. J.S.L. Leach and P. Neufeld, Corrosion Sci., 9, (1969) 413.
28. J.J. Randall and W.J. Bernard, Electrochim. Acta, 20 (1975) 653.
29. H. Takahashi and M. Nagayama, Electrochim. Acta, 23 (1978) 279.
30. Y.H. Choo and O.F. Devereux, J. Electrochem. Soc., 122, (1975) 1645.
31. T.P. Hoar and J. Yahalom, J. Electrochem. Soc., 110, (1963) 614.
32. J.P. O'Sullivan, Ph.D. Thesis, University of Manchester (1968).
33. G. Bailey, Ph.D. Thesis, University of Manchester (1978).
34. G.E. Thompson, R.C. Furneaux, G.C. Wood, J.A. Richardson and J.S. Goode, Nature, London, 272, (1978) 433.
35. Z.E. Thompson, R.C. Furneaux, J.S. Goode and G.C. Wood, Trans. Inst. Metal Finish., 56, (1978) 159.
36. G. Tu, Ph.D. Thesis, University of Manchester (1981).
37. G.E. Thompson, G.C. Wood and R.J. Hutchings, Trans. Inst. Metal Finish., 58, (1980) 21.
38. G.E. Thompson, R.C. Furneaux and G.C. Wood, Trans. Inst. Metal Finish, 55, (1977) 117.
39. P. Neufeld and H.O. Ali, Trans. Inst. Metal Finish., 47, (1969) 171.
40. P. Neufeld and H.O. Ali, Trans. Inst. Metal Finish., 48, (1970) 175.
41. P. Neufeld and H.O. Ali, J. Electrochem. Soc., 120, (1973) 479.
42. G. Bailey and G.C. Wood, Trans. Inst. Metal Finish., 52, (1974) 187.
43. S. Setoh and A. Miyata, Bull. Inst. Phys. Chem. Res., 11 (1932) 317.
44. F. Keller, M.S. Hunter and D.L. Robinson, J. Electrochem. Soc., 100, (1953) 411.
45. J.P. O'Sullivan and G.C. Wood, Proc. Royal Soc. London, A317, (1970) 511.
46. M.S. Hunter and P. Fowle, J. Electrochem. Soc., 101, (1954) 481.
47. M.S. Hunter and P. Fowle, J. Electrochem. Soc., 101, (1954) 514.
48. G. Paolini, M. Masaero, F. Sacchi and M. Paganelli, J. Electrochem. Soc., 112, (1965) 32.
49. R.B. Mason, J. Electrochem. Soc., 102, (1955) 671.
50. C.J.L. Booker, J.L. Wood and A. Walsh, Nature, London, 176, (1955) 222.
51. C.J.L. Booker, J.L. Wood and A. Walsh, Brit. J. Appl. Phys., 8, (1957) 347.
52. J.F. Murphy and C.E. Michelson, Proc. Symp. of Anodizing Aluminium, Nottingham University (1961) A.D.A., London p.83 (1962).
53. P. Csokan, Trans. Inst. Metal Finish., 41, (1964) 51.
54. P. Csokan, Electroplating and Met. Finish.,

- 15, (1962) 75.
55. T.A. Renshaw, *J. Electrochem. Soc.*, *108*, (1961) 185.
56. H. Ginsberg and K. Wefers, *Metall.*, *16*, (1962) 173.
57. H. Ginsberg and K. Wefers, *Metall.*, *17*, (1963) 202.
58. G.C. Wood and J.P. O'Sullivan, *Electrochim. Acta*, *15*, (1970) 1865.
59. N.D. Tomashov and F.D. Zalivalov, *Russ. J. Phys. Chem.*, *34*, (1961) 1709.
60. L.A. Cosgrove, *J. Phys. Chem.*, *60*, (1956) 385.
61. R.L. Burwell and T.P. May, *J. Electrochem. Soc.*, *94*, (1948) 195.
62. T.P. Hoar and N.F. Mott, *J. Phys. Chem. Solids*, *9*, (1959) 97.
63. H. Takahashi, M. Nagayama, H. Akahori and A. Kitahara, *J. Electron Microscopy*, *22*, (1973) 149.
64. G.E. Thompson and G.C. Wood, *Trans. Inst. Metal Finish.*, *58*, (1980) 21.
65. S. Ono, S. Chiaki and T. Sato, *Surf. Finish. Tech. of Metals*, *26*, (1975) 416.
66. G.E. Thompson, R.C. Furneaux and G.C. Wood, *Corrosion Sci.*, *18*, (1978) 481.
67. S.H. Tan, Ph.D Thesis, University of Manchester (1982).
68. J.W. Diggle, T.C. Downie and C.W. Goulding, *J. Electrochem. Soc.*, *116*, (1969) 737.